Electrochemistry Investigation on Protein Protection by Alkanethiol Self-Assembled Monolayers against Urea Impact

Yan Guo,[†] Jianwei Zhao,*[,†] Xing Yin,[†] Xiaoling Gao,[‡] and Yanni Tian[‡]

Key Laboratory of Analytical Chemistry for Life Science, School of Chemistry and Chemical Engineering, Nanjing University, 210093, Nanjing, P. R. China and Institute of Molecular Science, Shanxi University, 030006, Taiyuan, P. R. China

Received: October 3, 2007; In Final Form: January 22, 2008

The present investigation reports the electrochemical measurements of azurin (Az) adsorbed on a series of alkanethiol self-assembled monolayers (SAMs) under the influence of urea molecules. Theoretical fitting with the Marcus model obtains the electron-transfer rate constant, k_{et}, and the reorganization energy, λ. When the underlying SAM is longer than 10 methylene units, k_{et} shows an obvious chain-length dependence from which an electron-tunneling coefficient, β, of 1.09 per methylene is deduced. Combined with cyclic voltammetric results, variations of both k_{et} and λ imply that urea impact does not penetrate into the ion core part of Az but instead influences the network of molecular hydrogen bonds. The mechanism of urea impact is further discussed by means of the pH dependence of the equilibrium potential.

Introduction

Adsorption of proteins at liquid/solid interfaces is a primary event in many biological processes because many proteins are located in biomembranes, performing their biological activities, from respiration to energy conversion, in vivo. Using an organic self-assembled monolayer (SAM) to simulate the native biomembrane is an alternative strategy in the protein biomimic since organic SAM has a well-ordered and closely packed structure.[1,2] Systematic studies of the electron-transfer behavior of the redox protein on the SAM-modified metal electrode have attracted much attention, and these studies may contribute to a better understanding of the biological redox reactions and enable the development of new technologies in bioelectronics and biosensors.[3,4]

As evidenced from the surface electrochemistry, the existence of the organic layer may retain the structure and bioactivity of the adsorbed protein against the strong chemical interaction from the metal substrate.[1] However, the protein is rather large and soft as compared to the underlying layer and, therefore, prone to be distorted even by the supporting monolayer through van der Waals interaction.[3,5,6]

On the other hand, the structural rearrangement of protein is of great importance in some biological processes.[7−9] For example, the partially deformed metalloprotein, azurin, may keep the copper center in an appropriate position so that resonant electron tunneling can take place.[10−13] However, extreme deformation may lead to denaturation and loss of bioactivity.[10,12] Protein denaturation induced by urea in aqueous solutions has been carried out by numerous experimental and theoretical studies, though in the live body, many proteins are supported by membranes. Two main mechanisms have been proposed to interpret the denaturation process. One is attributed to the direct attack of urea on the peptide backbone and/or the residues, destroying the hydrogen-bonding network in the protein backbone.[14−19] The other is that the effective solvation of urea changes the structure of the water's hydrogen bond around hydrophobic groups, thereby increasing their solubility and weakening the hydrophobic effect.[20−25]

In the face of many solution-phase proteins denaturation studies, great concern grows about how denaturants affect proteins when supported by biomembranes and about how their heterogeneous electron-transfer kinetics varies. When adsorbed, the same protein even can have different conformations, showing different bioactivities and chemical properties.[26] Thus, detailed analysis of the adsorbed state of protein seems important in solving practical problems. Unfortunately, there are very few studies of the adsorbed protein denaturation because of the difficulty of studying the protein structure and function at a liquid/solid interface.

Azurin (Az), one of the blue copper proteins, functions as an electron shuttle in energy-conversion systems. It has been studied extensively for its structure, spectroscopic properties, and electron-transfer reactions.[27−31] Its copper ion is coordinated by two histidine imidazoles (His117 and His46) and one cysteine thiolate (Cys112) in a trigonal plane as well as two weaker axial (Met121 and Gly45) ligands forming a pseudotrigonal bipyramidal geometry.[32−35] Az can be immobilized directly on a metal surface via the disulfide group or in the opposite orientation via hydrophobic interactions with alkanethiol self-assembled monolayers (SAMs).[10,36−42] In the former case, azurin will gradually lose its activity due to the strong interaction with the metal electrode.[43] However, the later case is a good model to study the protein structure−activity relationship.[44]

In this paper, we employed alkanethiol monolayers to investigate how alkanethiol SAMs protect the adsorbed azurin against the urea effect (Figure 1). Cyclic voltammetry and impedance spectroscopy are used as electrochemical methods to probe the changes of the interfacial electron-transfer rate constant and reorganization energy. From the pH dependence

* To whom correspondence should be addressed. Phone/Fax: +86-25-83596523. E-mail: Zhaojw@nju.edu.cn.
[†] Nanjing University.
[‡] Shanxi University.

10.1021/jp7096668 CCC: $40.75
Published on Web 03/26/2008

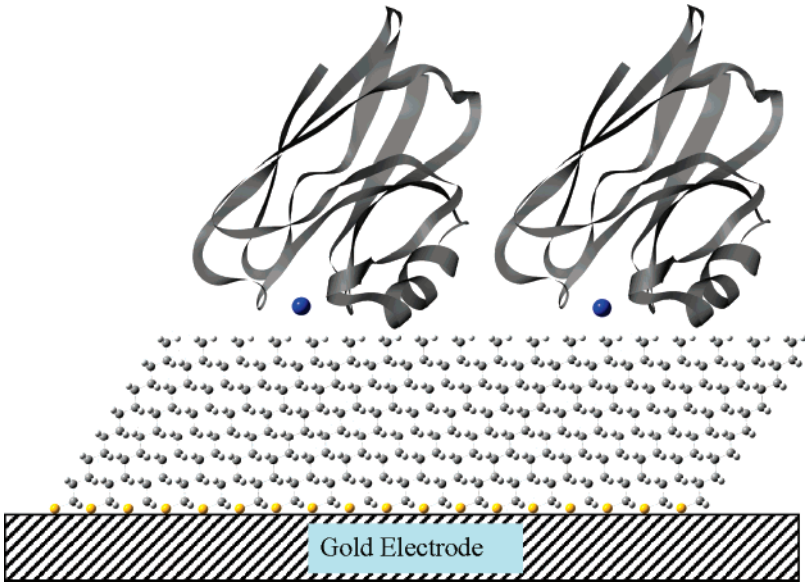

Figure 1. Schematic representation of Az on alkanethiol-modified Au electrode. This scheme is not drawn to scale.

of the electrochemical behavior and contact angle measurement, the influence of urea on adsorbed Az has been discussed as well.

Experimental Section

1. Reagents. *P. aeruginosa* azurin was purchased from Fluka. The Az solution was prepared with a 5.0 mM NH_4AC buffer solution (pH = 4.6, adjusting pH with $HClO_4$). The concentration was determined by UV−vis spectroscopy (Shimadzu UV3600) using a molar absorption coefficient of 5700 M^{-1} cm^{-1} at 628 nm.[45] 1-Butanethiol (HSC_4), 1-octanethiol (HSC_8), 1-decanethiol (HSC_{10}), 1-dodecanethiol (HSC_{12}), *n*-tetradecyl mercaptan (HSC_{14}), and 1-octadecanethiol (HSC_{18}) were purchased from Alfa Aesar and used as received. Urea (high purity, ≥99.0%) was purchased from the Shanghai Laser Fine Chemicals Factory, China. All other chemicals used were of analytical grade without further purification. All aqueous solutions were prepared with superpure water (>18.0 MΩ·cm, Millipore Corp.).

2. Electrode Preparation. The polycrystalline gold disk electrode (2.0 mm diameter, CHI 101, CHI Instruments) was sequentially polished with 1.0, 0.3, and 0.05 μm α-Al_2O_3 powder and rinsed thoroughly with superpure water. Then the gold electrode was electrochemically cleaned by potential cycling in 0.1 M H_2SO_4 in the potential range between −0.2 and 1.5 V until the typical cyclic voltammogram (CV) of clean gold was obtained. The real surface area of the gold electrode was determined by integration of the cathodic peak of CV during the reduction of superficial AuO. The charge of 0.386 mC cm^{-2} was accepted as the charge necessary to form a monolayer of electrosorbed O in the form of AuO.[46,47] The roughness factor of Au electrodes, calculated as the ratio between the real and the geometric surface area, was in the range between 1.2 and 1.4.

After rinsing with superpure water and ethanol, the gold electrodes were immersed in 1 mM alkanethiol solutions at room temperature for over 12 h to produce a self-assembled monolayer of alkanethiols. After copious rinsing with ethanol and superpure water, the electrodes were transferred to the 5.0 mM NH_4Ac buffer (pH = 4.6) with 100−250 μM Az for 6 h. Then the electrode was thoroughly rinsed with the NH_4Ac buffer before the electrochemical experiment. As for the urea effect, the azurin-modified electrodes were immerged into the 5.0 mM NH_4Ac buffer (pH = 4.6) with different urea concentrations for over 12 h. In order to compare the urea impact on Az in the solution, alkanethiol-modified electrodes were immersed in the Az buffer solution (5.0 mM NH_4Ac, pH = 4.6), which was treated first with urea for 12 h.

3. Electrochemical and Contact Angle Measurements. All electrochemical experiments were carried out using a conventional three-electrode cell with the modified gold electrode as the working electrode, a platinum wire as the auxiliary electrode, and a saturated calomel electrode (SCE) as the reference electrode. The cell was placed in a grounded Faraday cage. Electrolyte solutions (25.0 mM NH_4Ac buffer) were deoxygenated by purified nitrogen, and a nitrogen atmosphere was maintained over the solutions during the experiments. All electrochemical experiments were carried out at 0 °C. All potentials were given with respect to SCE. Cyclic voltammetry and ac impedance spectroscopy were performed on a CHI 660B electrochemical workstation (Shanghai Chenhua Apparatus Corp., China) and the Autolab system (PGSTAT 12), respectively. Under steady-state conditions, ac impedance spectra were recorded in the frequency range from 0.001 Hz to 100 kHz using an ac voltage of 5 mV amplitude. Using EIS, the solution resistance was obtained at 550 ± 30 Ω, so the *iR* drop is estimated to be less than 0.02 mV for HSC_4 SAM at a scan rate of 0.1 V s^{-1}, which can be ignored. A fast scan rate enlarged the influence of the *iR* drop. For example, at a scan rate of 100 V s^{-1}, the *iR* drop was estimated to be 5 mV. For pH-dependent experiments, a 50.0 mM phosphate buffer solution (PBS) with pH value varying from 4 to 10 was used as the electrolyte.

Evaporated gold film was used for the contact angle measurement. It was exposed to a piranha solution for 5 min (3:1 H_2SO_4:30% H_2O_2), then washed with copious amounts of superpure water, and washed again with redistilled ethanol before immersion. Contact angle measurements were carried out with a JJC-I contact angle goniometer (Changchun fifth Optical Instrument, China).

Results and Discussion

Electrochemistry of Az-Modified Electrode. To reveal the urea effect, we first characterized the Az/SAM-modified electrode. Figure 2A shows the typical CVs of Az adsorbed on the HSC_8–Au electrode at scan rates ranging from 0.01 to 0.5

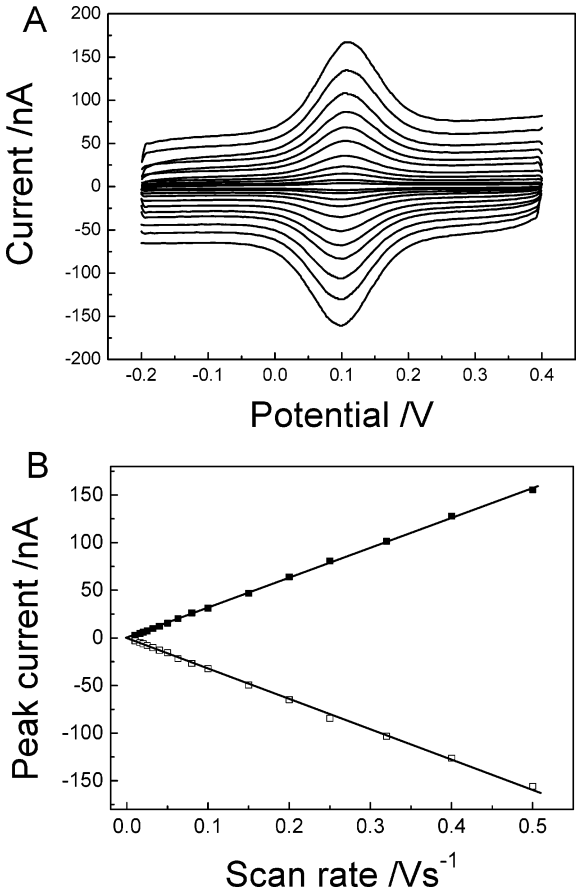

Figure 2. (A) Cyclic voltammograms of Az on $HSC_{8-}Au$ electrode in 25 mM NH_4Ac (pH = 4.6) solution at scan rates of 0.01, 0.02, 0.04, 0.063, 0.10, 0.15, 0.20, 0.25, 0.32, 0.40, and 0.5 V s^{-1}. The temperature is 273 K. (B) Linear relations of the anodic and cathodic peak currents versus scan rates.

V s^{-1}. Figure 2B is the linear relationship of the peak current with the scan rate, confirming the characteristic surface-confined electrochemical process according to eq 1[48]

$$i = \frac{nFAQv}{4RT} \tag{1}$$

where n is the number of moles of electrons transferred, F is the Faraday constant (F = 96485 C mol^{-1}), A is the electrode surface area (cm^2), Q is the charge involved in the electrochemical process (C), and v is the scan rate (V s^{-1}), R is the molar gas constant (R = 8.314 J mol^{-1} K^{-1}) and T is the temperature (in Kelvin). The voltammetric waves are symmetric, and the separation between the oxidation and the reduction peaks (ΔE_p) is less than 10 mV, indicating that the electron-transfer process is rather rapid and reversible. The apparent formal potential, $E^{\circ\prime}$ (determined from the mean of the oxidation and reduction peak potentials), is about 0.095 mV, very close to those reported previously, though different electrolyte and higher temperatures are used.[37,39,49] The full-width at half-maximum of the anodic voltammetric wave, ΔE_{fwhm}, is about 0.092 ± 0.002 V, slightly larger than the value of 0.083 V according to the ideal one-electron process at 273 K ($3.53RT/nF$).[50]

The Az-modified electrode reacted further with urea in the buffer solution at concentrations of 3.0, 6.0, and 9.0 M. Figure 3 gives CVs of Az on alkanethiol SAMs (HSC_n-Au, n = 8 and 14), and Figure S1 (in Supporting Information) gives other CVs on HSC_n-Au (n = 4, 10, 12, and 18) before and after the urea effect. All electrochemical characterizations were carried

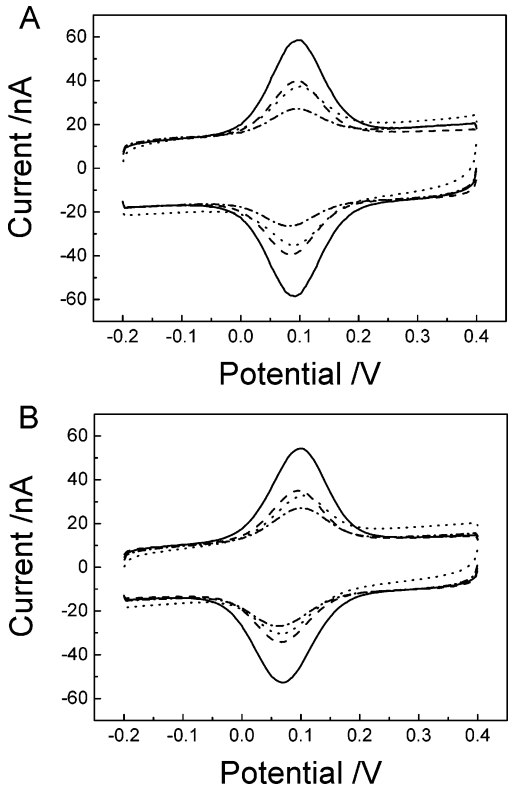

Figure 3. Cyclic voltammograms of Az on HSC_n-Au (n = 8 (A) and 14 (B)) electrodes before and after the urea effect, respectively. Curve, solid (without urea); urea concentration, dash (3.0 M), dot (6.0 M), and dash dot (9.0 M). The temperature is 273 K. Electrolyte: 25 mM NH_4Ac (pH = 4.6). Scan rate: 0.1 V s^{-1}.

out at a pH of 4.6. At this value the disturbance to apparent formal potential that comes from other moieties is less, and this point will be discussed in detail later. The most important CV features, e.g., $E^{\circ\prime}$, ΔE_p, ΔE_{fwhm}, and Γ (the surface coverage (mol cm^{-2})), are summarized in Table 1. Due to the potential drop within the monolayer,[51] $E^{\circ\prime}$ shifts negatively as a function of the methylene number. ΔE_p is a qualitative indicator for a heterogeneous electron-transfer rate. When n is less than 10, there is no obvious change in ΔE_p while there is also no urea interaction. However, ΔE_p increases when n is larger than 10, reflecting the dependence of electron transfer on the methylene number. We also noted fluctuation of the surface coverage among the samples with different chain lengths. The protein coverage on a moderate chain length looks larger than those either on thicker or thinner SAMs. Similar observations have also been reported by Ulstrup et al., showing an increase of surface coverage followed by a decrease with an increase in the monolayer thickness.[39] However, while a mixed monolayer of alkanethiol and ω-hydroxy-alkanethiol is used, only a monotonic decrease of protein surface coverage was found as shown in Leigh's report.[52] From these results one can speculate the role of the interfacial interaction. In the system of alkanethiol monolayers, the surface hydrophobicity is intensified, facilitating Az adsorption, with the increase of the chain length, as proved by our (Table S1) and previous contact angle measurement.[53] Though the hydrophobic interaction is essentially required to fix the protein molecules, other factors may also lead to some negative effects, for example, the protein structural rearrangement and the rigidity of SAM.

The variation of electrochemical behavior before and after the urea impact may give insight into the molecular interaction and the role of the supporting monolayer. From Figure 3 and Table 1 we can see that after the urea impact on the surface,

TABLE 1: Apparent Formal Potential ($E^{\circ\prime}$) of Az on HSC_n−Au (n = 4, 8, 10, 12, 14, and 18) Electrodes[a]

		Az/HSC_4	Az/HSC_8	Az/HSC_{10}	Az/HSC_{12}	Az/HSC_{14}	Az/HSC_{18}
E°/V		0.105 ± 0.002	0.095 ± 0.004	0.091 ± 0.002	0.086 ± 0.003	0.089 ± 0.002	0.081 ± 0.004
ΔE_p/V	original	0.011 ± 0.003	0.010 ± 0.004	0.008 ± 0.001	0.018 ± 0.004	0.030 ± 0.002	0.281 ± 0.015
	3.0 M urea	0.016 ± 0.004	0.012 ± 0.002	0.008 ± 0.002	0.018 ± 0.003	0.030 ± 0.003	0.292 ± 0.024
	6.0 M urea	0.023 ± 0.004	0.012 ± 0.003	0.010 ± 0.002	0.025 ± 0.005	0.036 ± 0.004	0.300 ± 0.035
	9.0 M urea	0.029 ± 0.006	0.016 ± 0.003	0.012 ± 0.002	0.033 ± 0.003	0.040 ± 0.005	0.305 ± 0.028
ΔE_{fwhm}/V	original	0.095 ± 0.004	0.092 ± 0.007	0.095 ± 0.003	0.097 ± 0.010	0.106 ± 0.006	0.162 ± 0.014
	3.0 M urea	0.097 ± 0.003	0.093 ± 0.005	0.095 ± 0.005	0.099 ± 0.005	0.098 ± 0.008	0.160 ± 0.020
	6.0 M urea	0.090 ± 0.004	0.091 ± 0.003	0.095 ± 0.002	0.094 ± 0.004	0.096 ± 0.004	0.156 ± 0.015
	9.0 M urea	0.088 ± 0.006	0.088 ± 0.007	0.092 ± 0.004	0.090 ± 0.008	0.096 ± 0.005	0.155 ± 0.028
$\Gamma/10^{-12}$ mol cm^{-2}	original	4.6 ± 0.8	6.2 ± 0.9	9.1 ± 1.1	5.8 ± 0.7	7.0 ± 0.4	2.9 ± 0.9
	3.0 M urea	2.7 ± 0.5	3.7 ± 0.7	5.0 ± 0.7	3.3 ± 0.6	3.8 ± 0.4	1.7 ± 0.4
	6.0 M urea	1.4 ± 0.3	3.1 ± 0.6	2.8 ± 0.5	2.2 ± 0.4	2.8 ± 0.4	1.1 ± 0.2
	9.0 M urea	0.92 ± 0.13	1.9 ± 0.4	2.2 ± 0.4	1.6 ± 0.3	2.1 ± 0.2	0.93 ± 0.29

[a] The oxidation and reduction peak potentials (ΔE_p), full-width at half-maximum of the anodic voltammetric wave (ΔE_{fwhm}), and surface coverage (Γ) of Az on HSC_n–Au (n = 4, 8, 10, 12, 14, and 18) electrodes before and after the urea effect with concentrations of 3.0, 6.0, and 9.0 M.

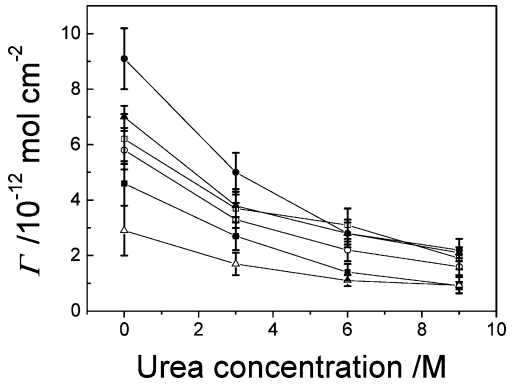

Figure 4. Change of Γ for Az on HSC_n−Au (n = 4 (■), 8 (□), 10 (●), 12 (○), 14 (▲), and 18 (□)) electrodes with urea concentrations of 0, 3.0, 6.0, and 9.0 M. Γ is normalized by the value without urea effect for each sample.

electrochemical features are not changed significantly except for the peak current for all samples, whereas for urea impact in a solution the peak current is much lower (Figures S2, S3, and S4) and the CV features almost disappear for high urea concentration. This observation implies a difference in the impact of urea on Az on the surface and in solution. It is much more intense for the later. For previous denaturation experiments in solutions, UV and circular dichroism spectroscopy showed that Az may lose its characteristic absorption under 6.0 M urea interaction.[57−59] In addition, when protein is denatured in solution, the formal potential may greatly shift positively.[60−62] The formal potential is, to a certain extent, related to the coordination environment of Cu center[54−56] and the negligible change of the $E^{\circ\prime}$ value when adsorbed, even under the impact of 9.0 M urea, implying that the urea effect does not reach the core part of Az. From the comparison of protein electrochemistry made in solution and on the surface, one can infer that the underlying alkanethiol monolayer may support Az against denaturation by urea.

Although the urea does not directly impact the Cu center, its influence can be reflected in terms of ΔE_p, ΔE_{fwhm}, and Γ. ΔE_p increases and ΔE_{fwhm} decreases, though the variation is not so obvious. In a blank experiment for the same condition without urea, loss of surface coverage is less than 5%, indicating that Az is quite stable on the hydrophobic surface. However, treatment with urea solution greatly decreases the surface coverage. Figure 4 gives the coverage of those remaining active proteins as a function of urea concentration. Since the loss of protein coverage is irreversible, we propose that the urea impact may reduce the hydrophobic interaction between protein and SAMs. In order to obtain the entire picture of the urea effect, we will further examine the electron-transfer rate and reorganization energy.

Electron-Transfer Rate of Az-Modified Electrode. Electrochemical impedance is employed in the present work. Due to the limited amount of redox molecules on the surface, the impedance spectrum differs significantly from the diffusion-controlled redox species.[63] The equivalent circuit is shown in Figure 5A, including the ohmic resistance of the electrolyte solution, R_s, the capacitance of double-layer, C_{dl}, the resistance of electron-communication resistance, R_{ec}, and the pseudocapacitance, C_{pc}, corresponding to the electrochemical charging/discharging process of the surface-confined redox species. For the surface-confined redox systems, the electrochemical impedance spectra are usually presented in the form of Cole−Cole plots, particularly in the form of C_{im} vs C_{re} (where C_{im} and C_{re} are imaginary and real parts of the interfacial complex capacitance, respectively) as suggested.[63−65] The Cole−Cole presentation describes the distribution of relaxation processes corresponding to the charging of the monolayer. The imaginary and real parts of the capacitance (C_{im} and C_{re}) can be described in terms of the imaginary and real parts of the impedance Z

$$C_{im} = -\mathrm{Im}[(j\omega Z)^{-1}] \quad (2)$$

$$C_{re} = \mathrm{Re}[(j\omega Z)^{-1}] \quad (3)$$

Figure 5B presents the impedance spectra of Az on HSC_n−Au (n = 4, 8, 10, 12, 14, and 18) electrodes in the form of Cole−Cole plots. The nonfaradaic semicircle at high frequencies corresponds to the double-layer capacitance C_{dl}, the diameter of which is in a reciprocal proportion with the number of carbon chains. The faradaic semicircle at low frequencies is for the pseudocapacitance, C_{pc}. The electron-transfer rate constant, k_{et}, can be derived from the frequency, f°, corresponding to the maximum value of pseudocapacitance C_{pc}[64]

$$k_{et} = \pi f^{\circ} \quad (4)$$

For short SAMs (HSC_n−Au, n = 4, 8, and 10), the time constants, $\tau = RC$, of nonfaradaic and faradaic processes are similar. As a result, the semicircle at low frequency is covered by the larger one contributed by the high-frequency signal, and therefore, the two processes cannot be separated on the Cole−Cole plots. When the monolayer is thick enough (n = 12, 14, and 18), two semicircles are observed; from the one at high frequency, the electron-transfer rate k_{et} can be derived based on eq 4 as given in Table 2.

In the EIS plot (Figure 5C), there is no significant difference observed for semicircles at high frequency, indicating that the

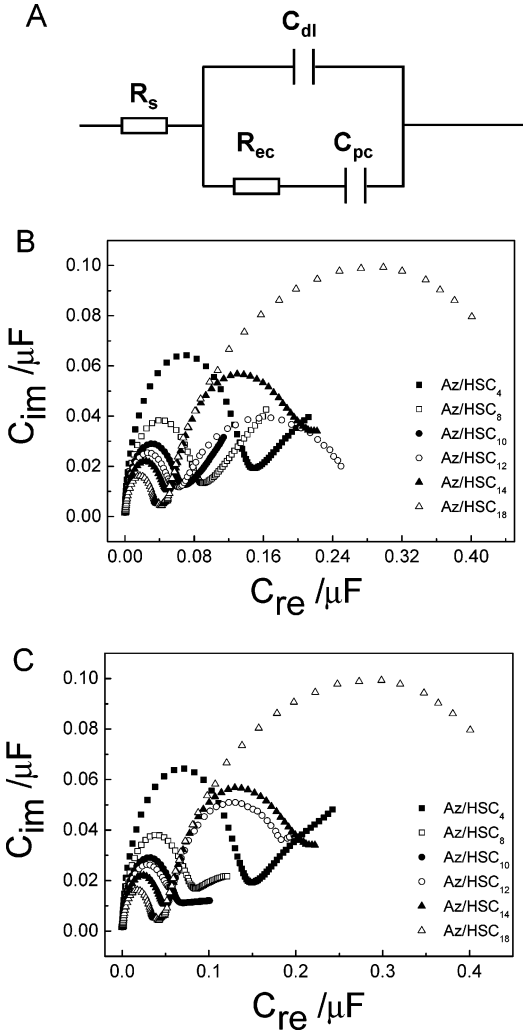

Figure 5. (A) Equivalent circuit for a Faradaic impedance spectrum corresponding to a surface-confined species. Impedance spectra of Az on HSC_n−Au (n = 4 (■), 8 (□), 10 (●), 12 (○), 14 (▲), and 18 (□)) electrodes before (B) and after (C) the urea effect in the form of Cole−Cole plots. The temperature is 273 K. Electrolyte: 25 mM NH_4Ac (pH = 4.6).

double layer does not change even after urea treatment, whereas for semicircles at low frequency (for n = 12, 14, and 18) the plots present a dramatic decrease of C_{pc}, which comes from the decrease of surface coverage,[63,64] as also proved by the CV measurement. k_{et} decreases as well with the decrease of $f°$.

Another approach to estimate the electron-transfer rate constant is from the peak separation as proposed by Laviron with the classic Butler−Volmer relation.[66] In the last two decades, the Marcus model has been used widely for long-range heterogeneous electron transfer, which considers the contribution of the reorganization energy to the electron-transfer rate. According to the semiclassical Marcus model, the k_{et} for a nonadiabatic system can be written as[67−69]

$$k_{et} = \frac{2\pi}{\hbar}|H_{AD}|^2 \frac{1}{\sqrt{4\pi\lambda k_B T}} \exp\left[-\frac{(\lambda + (\epsilon_F - \epsilon) + e\eta)^2}{4\lambda k_B T}\right] \quad (5)$$

where H_{AD} is the electronic coupling element, which is a function of the overlap of the wave functions of the two states involved in the reaction. It depends on the delocalization of the electron to be transferred in the metal site and the protein matrix between the two active sites. λ is the reorganization energy, i.e., the energy associated with relaxing the geometry of the system after electron transfer. It can be divided into two parts: inner-sphere reorganization energy (λ_{ir}) and outer-sphere reorganization energy (λ_{or}), depending on which atoms are relaxed. For azurin, the inner-sphere reorganization energy is associated with the structural change of the first coordination sphere and the outer-sphere reorganization energy involves the structural change of the remaining protein as well as the solvent. ϵ_F is the Fermi level of the electrode, i.e., the applied potential. ϵ is the energy of a given state in the electrode, and η is the overpotential, i.e., the applied potential relative to the formal potential.

Figure 6 is the dependence of peak potential on the natural logarithm of scan rate for Az on HSC_n−Au (n = 8 and 14) (others on HSC_n−Au (n = 4, 10, 12, and 18) are shown in Figure S5) electrodes before and after the urea effect with different concentrations of 3.0, 6.0, and 9.0 M, respectively. The data points are obtained from CV plots; the lines are theoretically fitted with eq 5 using a self-written program.[70] The detailed k_{et} values derived from Laviron's formalism and the Marcus model are summarized in Table 2. Results derived from the Marcus model are similar to that from EIS but less than that from Laviron's formalism, consistent with the fact that Butler−Volmer theory is an approximation while λ is the infinity in the Marcus model.

Interestingly, after urea interaction, k_{et} displays a substantial increase for the protein on short alkyl SAMs, whereas it decreases or remains approximately constant for long alkyl SAMs. At present, we cannot give a specific explanation for this phenomenon. However, we speculate that the increased electron-transfer rate on thin films is related to the microstructure of the SAM. As evidenced by the large charging capacitance, one can expect that the thin SAM has a loose structure. The existence of many defects and pin holes allows for penetration of urea molecules into the microstructure of SAM, leading to a change of the microenvironment around the protein. This is probably the reason for the increased electron-transfer rate of Az on the thin SAM.

TABLE 2: Electron-Transfer Rate, k_{et}, of Az on HSC_n−Au (n = 4, 8, 10, 12, 14, and 18) Electrodes Derived from Impedance Spectra (Figure 5) and Cyclic Voltammetry (Figure 6 and Figure S5) Using Laviron's Formalism and the Marcus Model, Respectively

		Az/HSC_4	Az/HSC_8	Az/HSC_{10}	Az/HSC_{12}	Az/HSC_{14}	Az/HSC_{18}
k_{et}/s^{-1} (EIS)	original				54 ± 4	7.8 ± 1.0	0.08 ± 0.01
	6.0 M urea				42 ± 5	6.2 ± 0.8	0.07 ± 0.01
k_{et}/s^{-1} (CV)	original	850 ± 90	650 ± 40	360 ± 40	94 ± 15	9.9 ± 1.7	0.20 ± 0.02
	3.0 M urea	920 ± 50	730 ± 120	370 ± 50	85 ± 12	8.9 ± 0.8	0.20 ± 0.03
	6.0 M urea	970 ± 100	810 ± 80	420 ± 30	78 ± 15	7.8 ± 2.0	0.19 ± 0.03
	9.0 M urea	1060 ± 150	920 ± 130	490 ± 80	66 ± 8	7.0 ± 1.0	0.17 ± 0.02
k_{et}/s^{-1} (simulation)	original	590 ± 60	450 ± 30	270 ± 30	60 ± 10	6.4 ± 1.1	0.05 ± 0.005
	3.0 M urea	680 ± 40	530 ± 90	290 ± 40	56 ± 7	6.2 ± 0.5	0.05 ± 0.008
	6.0 M urea	800 ± 90	630 ± 60	320 ± 30	50 ± 10	5.9 ± 1.5	0.05 ± 0.007
	9.0 M urea	900 ± 120	750 ± 100	360 ± 60	45 ± 5	5.2 ± 0.7	0.04 ± 0.005

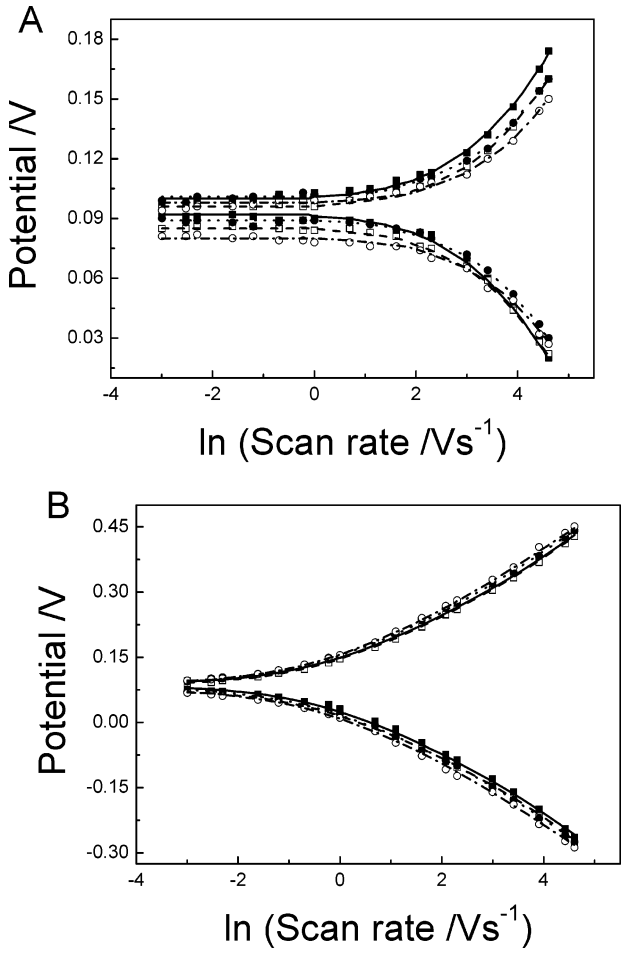

Figure 6. Peak potential as a function of the natural logarithm of the scan rate for Az on HSC_n−Au ($n = 8$ (A) and 14 (B)) electrodes before and after the urea effect, respectively. Data, without urea (■); urea concentration, 3.0 M (□), 6.0 M (●), and 9.0 M (○). Curves are fits to eq 5 described in the text: without urea (solid); urea concentration, 3.0 M (dash), 6.0 M (dot), and 9.0 M (dash dot). The temperature is 273 K. Electrolyte: 25 mM NH_4Ac (pH = 4.6).

For long-range electron transfer, an approximate expression is used to describe the distance dependence of k_{et} due to the electronic coupling parameter

$$k_{et} = A \exp(-n\beta) \tag{6}$$

where n is the number of methylene units, β is the electronic tunneling factor, and A is a constant.[71] k_{et} decreases exponentially as the alkyl chain has 10 or more methylene units as shown in Figure 7. From the slope, we get a β value of 1.09 per methylene unit, which is close to that for electron transfer between proteins, such as azurin and cytochrome *c* (Cyt-*c*), and the gold electrode along with the alkyl chains.[39,52,72,73] We also noted that when the urea concentration changes from 0 to 9.0 M, β varies between 1.09 and 1.14 per methylene with minor fluctuation. k_{et} for a short alkyl chain is nearly distance independent, consistent with the previous observation.[39,52,72−74] However, these distance-independent phenomena are not observed for alkanethiols, alkanedithiols, ferrocene-terminated thiols, and hydroquinone-terminated thiol systems,[75−77] which have redox moieties covalently bonded to the alkyl chains. These kinetic gated behaviors have been associated with the conformationally gated mechanism related to the nuclear rearrangement.[73,78,79] However, one limitation of this mechanism is that the electron transfer does not obey the Marcus model on short

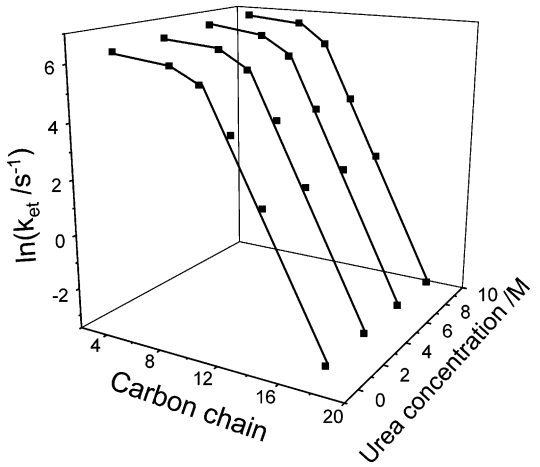

Figure 7. Plots of the number of carbon chains and urea concentration dependence of the electron-transfer rate k_{et}. k_{et} is obtained from fits of the Marcus model (Table 2). β obtained from the slope is 1.09, 1.10, 1.12, and 1.14 with a corresponding urea concentration of 0, 3.0, 6.0, and 9.0 M.

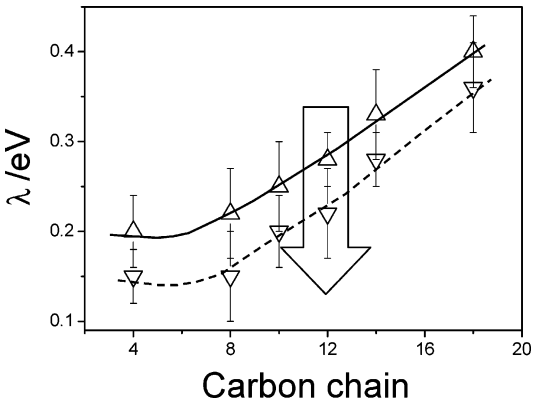

Figure 8. Change of the reorganization energy λ for Az on HSC_n−Au ($n = 4$, 8, 10, 12, 14, and 18) electrodes before (up triangle) and after (down triangle) 9.0 M urea effect. λ is obtained from Marcus fits using eq 5 described in the text.

alkyl chains. More recently, Waldeck et al. used a friction-controlled mechanism concerned with electronic coupling and polarization relaxation to explain this kinetic gating. A more detailed discussion is given in ref 74.

Reorganization Energy of Az-Modified Electrode. Theoretical fitting using eq 5 may also give the reorganization energy, λ, as shown in Figure 8. The λ value of Az is small as compared with other redox species such as Cyt-*c* and ferrocene,[2,76,80,81] but it is similar to that reported by Ulstrup et al. using the chronoamperometric technique.[39,82] As estimated theoretically, the electrochemical center of Az has an atomic configuration between the tetrahedral coordination preferred by Cu(I) and the tetragonal geometry preferred by by Cu(II).[83,84] Theoretical prediction based on the entatic state and induced-rack theories also suggested that the protein forms a rigid structure, which forces the Cu(II) ion into a coordination sphere more similar to that preferred by Cu(I).[85−88] As a result, no considerable geometric change takes place during protein reduction, producing a small reorganization energy and allowing a fast electron transfer.[71,89] The reorganization energy increases about 2-fold when the underlying SAM increases from $n = 4$ to 18. This observation implies a larger structural fluctuation of Az when a longer SAM is used. It is clear that the longer SAM is more hydrophobic as proven by the contact angle measurement. Therefore, the longer SAM may provide more effective protection against the rearrangement of protein, leading to higher

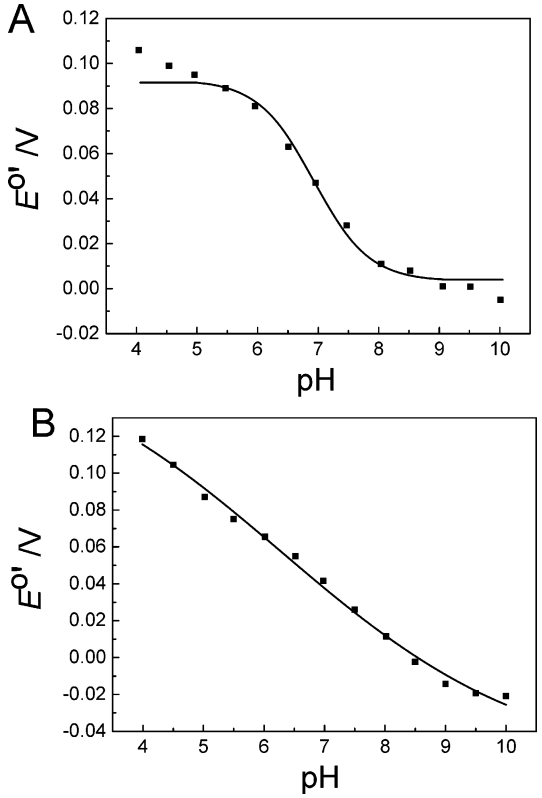

Figure 9. Change of the formal potential of Az on $HSC_{8-}Au$ (determined as the midpoint potential from cyclic voltammograms at 0.1 V s^{-1}) with the pH of buffer solution (pH 4−10, 50 mM PBS buffer) before (A) and after (B) 6.0 M urea effect. The solid line in Figure 9A is the fit to eq 7 described in the text.

reorganization energy. This explanation is consistent with the theoretical prediction by a continuum model.[90]

In the fitting with the Marcus model, λ is a nonsensitive parameter as also recognized by others.[74,81] In our study, there is no obvious difference in the fitting if the variation of λ is within $\pm$0.05 eV while keeping k_{et} the same. For the 3.0 and 6.0 M urea concentrations, the results fall into the fitting error and are not convincing. Therefore, we compare only the results of the 9.0 M urea effect. After the urea interaction, λ decreases for all samples but the amplitude is still small as compared with the fitting error. This implies that the urea effect is quite small. Furthermore, the slight decrease can be attributed to the change of λ_{out}. Previous quantum calculation and experimental studies also demonstrated that much of λ variation is associated with outer-sphere reorientation when there is an outside disturbance.[2,91−94] However, protein is a complex system, and even λ_{out} can be divided into several contributions,[95] such as the internal unconstrained water molecules, the surface polarization constraints, the harmonically constrained protein atoms, and the internal protein dielectric properties. One question is which particular part the urea effect can be assigned to. We speculate that the variation might be related to the change of the internal hydrogen bond of Az, which will be discussed later in detail.

Urea-Induced Internal Hydrogen-Bond Change. The mechanism of the denaturing effects of urea on proteins is still an unsolved and important problem in protein chemistry. The focus is on the pathways of how urea reacts with protein, directly or indirectly. The following experiments may shed some light on the mechanisms of urea-induced denaturation. Figure 9 is the typical dependence of formal potential of Az/HSC_8 on the pH of PBS electrolyte before (A) and after (B) 6.0 M urea effect. His35 and His83 of Az are mainly responsible for pH-dependent behaviors, which are located approximately 8 and 13 Å from the Cu site.[33,49] His83 is exposed to the solvent molecules on the surface, and its proton-transfer kinetics is very fast. Normally, its pK_a values are determined by NMR.[34,49] His35 is somewhat buried, and the proton-transfer kinetics is slower,[96,97] and from the pH-dependent potential change one can obtain its pK_a values. Before urea influence, the protonation−deprotonation process of His35 brought about a conformation change because His35 flips the Pro36-Gly37 peptide bond at different joint moieties at different pH conditions.[49,98] This process is reflected in Figure 9A as a sigmoid shape in the pH range of 5−9. The protonation−deprotonation of His35 can be expressed as follows[99]

$$E^0 = E^0_{\text{highpH}} - \frac{RT}{nF}\log\frac{10^{-\text{p}K_{\text{red}}}(10^{-\text{p}K_{\text{ox}}} + 10^{-\text{pH}})}{10^{-\text{p}K_{\text{ox}}}(10^{-\text{p}K_{\text{red}}} + 10^{-\text{pH}})} \quad (7)$$

The data in Figure 9A fit eq 7 well and give pK_{red} and pK_{ox} of His35 values of 7.3 $\pm$ 0.2 and 6.5 $\pm$ 0.1, respectively, very similar to former reports.[33,49,100] Because the protonation−deprotonation process of His35 will bring some conformation change, all other electrochemical characterizations are carried out at a pH of 4.6, which is quite a bit smaller than pK_{red} and pK_{ox} of His35, to reduce its influence. At higher or lower pH the data deviates from the fit, indicating that other amino acids also participate in the protonation−deprotonation process, though with minor contributions.

After the urea effect the sigmoidal shape is replaced by a line between pH 4 and 9. The linear relation is characteristic of a proton-involved redox process without conformation change, and the main involvement of the proton is to balance the excess surface charge accumulated at the interface. This change may be attributed to the hydrogen-bond effect of aminophenol active moieties with urea molecules and lose its sensitivity to protonation−deprotonation. Other pH-dependent measurements of Az/HSC_n (n = 4, 10, 12, 14, and 18) have produced similar results.

Conclusions

In this work, we used electrochemistry methods to study the urea effect on adsorbed Az on the SAM-modified gold electrode. Electrochemical results preliminarily indicate that urea influence cannot penetrate into the core part of Az. At the same time, length-dependent Az adsorption is expressed because of intensified hydrophobic interactions between Az and thiols as alkyl chain length increases. Consequently, different responses of k_{et} to the urea impact have been observed. By detailed analysis of the variations of k_{et} and λ, we find that urea only influences the network of molecular hydrogen bonds of Az, which is further discussed by the pH-dependent equilibrium potential. The importance of the underlying alkanethiol monolayer can be viewed as supporting Az against urea attack just like the protection of biomembranes for some proteins in nature.

Acknowledgment. This project was supported by the National Nature Science Foundation of China (Nos. 20503012, 20435010, and 20521503) and the Open Foundation of State Key Laboratory of Bioelectronics of Southeast University.

Supporting Information Available: Cyclic voltammograms for urea influence on Az when adsorbed on HSC_n−Au electrodes (n = 4, 10, 12, and 18); cyclic voltammograms for urea influence on Az in solution; comparisons of CVs for urea influence on the surface and in solution; peak potential as a

function of the natural logarithm of scan rate for urea influence on Az when adsorbed on HSC_n−Au electrodes ($n = 4$, 10, 12, and 18); tables of contact angle experiments. This material is available free of charge via the Internet at http://pubs.acs.org.

References and Notes

(1) Rusling, J. F. *Acc. Chem. Res.* **1998**, *31*, 363−369.
(2) Fedurco, M.; Augustynski, J.; Indiani, C.; Smulevich, G.; Antalík, M.; Bánó, M.; Sedlák, E.; Glascock, M. C.; Dawson, J. H. *J. Am. Chem. Soc.* **2005**, *127*, 7638−7646.
(3) Norde, W.; Haynes, C. A. *Proteins at Interfaces II, Fundamentals and Applications*; American Chemical Society: San Diego, CA, 1995.
(4) Adamson, A. W. *Physical Chemistry of Surfaces*, 5th ed.; John Wiley and Sons: New York, 1990.
(5) Karlsson, M.; Mårtensson, L. G.; Jonsson, B. H.; Carlsson, U. *Langmuir* **2000**, *16*, 8470−8479.
(6) Kanthimathi, M.; Maheshwari, R.; Dhathathreyan, A. *Langmuir* **2003**, *19*, 3398−3402.
(7) Wright, P. E.; Dyson, H. J. *J. Mol. Biol.* **1999**, *293*, 321−331.
(8) Radford, S. E.; Dobson, C. M. *Cell* **1999**, *97*, 291−298.
(9) Svensson, M.; Sabharwal, H.; Hakansson, A.; Mossberg, A. K.; Lipniunas, P.; Leffler, H.; Svanborg, C.; Linse, S. *J. Biol. Chem.* **1999**, *274*, 6388−6396.
(10) Zhao, J. W.; Davis, J. J.; Sansom, M. S. P.; Hung, A. *J. Am. Chem. Soc.* **2004**, *126*, 5601−5609.
(11) Zhao, J. W.; Wang, N. *Chem. J. Chin. Univ.* **2005**, *26*, 751−753.
(12) Davis, J. J.; Wang, N.; Morgan, A.; Zhang, T.; Zhao, J. *Faraday Discuss.* **2006**, *131*, 167−169.
(13) Maruccio, G.; Marzo, P.; Krahne, R.; Passaseo, A.; Cingolani, R.; Rin, R. *Small* **2007**, *3*, 1184−1188.
(14) Robinson, D. R.; Jencks, W. P. *J. Am. Chem. Soc.* **1965**, *87*, 2462−2470.
(15) Makhatadze, G. I.; Privalov, P. L. *J. Mol. Biol.* **1992**, *226*, 491−505.
(16) Myers, J. K.; Pace, C. N.; Scholtz, J. M. *Protein Sci.* **1995**, *4*, 2138−2148.
(17) Wallqvist, A.; Covell, D. G.; Thirumalai, D. *J. Am. Chem. Soc.* **1998**, *120*, 427−428.
(18) Mountain, R. D.; Thirumalai, D. *J. Am. Chem. Soc.* **2003**, *125*, 1950−1957.
(19) Tobi, D.; Elber, R.; Thirumalai, D. *Biopolymers* **2003**, *68*, 359−369.
(20) Wetlaufer, D. B.; Malik, S. K.; Stoller, L.; Coffin, R. L. *J. Am. Chem. Soc.* **1964**, *86*, 508−514.
(21) Hammes, G. G.; Schimmel, P. R. *J. Am. Chem. Soc.* **1967**, *89*, 442−446.
(22) Kuharski, R. A.; Rossky, P. J. *J. Am. Chem. Soc.* **1984**, *106*, 5794−5800.
(23) Zou, Q.; Habermann-Rottingaus, S. M.; Murphy, K. P. *Proteins* **1998**, *31*, 107−115.
(24) Shimizu, S.; Chan, H. S. *Proteins* **2002**, *49*, 560−566.
(25) Lee, M.-E.; van der Vegt, N. F. A. *J. Am. Chem. Soc.* **2006**, *128*, 4948−4949.
(26) Migueles, S. A.; Sabbaghian, M. S.; Shupert, W. L.; Bettinotti, M. P.; Marincola, F. M.; Martino, L.; Hallahan, C. W.; Selig, S. M.; Schwartz, D.; Sullivan, J.; Connors, M. *Proc. Natl. Acad. Sci. U.S.A.* **2000**, *97*, 2709−2714.
(27) Farver, O.; Pecht, I. *J. Am. Chem. Soc.* **1992**, *114*, 5764−5767.
(28) Farver, O.; Skov, L. K.; Van de Kamp, M.; Canters, G. W.; Pecht, I. *Eur. J. Biochem.* **1992**, *210*, 399−403.
(29) Farver, O. *Protein Electron Transfer*; BIOS Scientific Publishers: Oxford, 1996.
(30) Gray, H. B.; Winkler, J. R. *Annu. Rev. Biochem.* **1996**, *65*, 537−561.
(31) Winkler, J. R.; Gray, H. B. *J. Biol. Inorg. Chem.* **1997**, *2*, 399−404.
(32) Adman, E. T. *Adv. Protein Chem.* **1991**, *42*, 145−197.
(33) Nar, H.; Messerschmidt, A.; Huber, R.; van de Kamp, M.; Canters, G. W. *J. Mol. Biol.* **1991**, *221*, 765−772.
(34) Nar, H.; Messerschmidt, A.; Huber, R.; van de Kamp, M.; Canters, G. W. *FEBS Lett.* **1992**, *306*, 119−124.
(35) Gray, H. B.; Solomon, E. I. *Copper proteins*; John Wiley and Sons: New York, 1980; Vol. 3.
(36) Axford, D.; Davis, J. J.; Wang, N.; Wang, D.; Zhang, T.; Zhao, J.; Peters, B. *J. Phys. Chem. B* **2007**, *111*, 9062−9068.
(37) Gaigalas, A. K.; Niaura, G. *J. Colloid Interface Sci.* **1997**, *193*, 60−70.
(38) Chi, Q.; Zhang, J.-D.; Nielsen, J. U.; Friis, E. P.; Chorkendorff, I.; Canters, G. W.; Andersen, J. E. T.; Ulstrup, J. *J. Am. Chem. Soc.* **2000**, *122*, 4047−4055.
(39) Chi, Q.; Zhang, J.-D.; Andersen, J. E. T.; Ulstrup, J. *J. Phys. Chem. B* **2001**, *105*, 4669−4679.
(40) Jeuken, L. J. C.; Armstrong, F. A. *J. Phys. Chem. B* **2001**, *105*, 5271−5282.
(41) Jeuken, L. J. C.; McEvoy, J. P.; Armstrong, F. A. *J. Phys. Chem. B* **2002**, *106*, 2304−2313.
(42) Armstrong, F. A.; Barlow, N. L.; Burn, P. L.; Hoke, K. R.; Jeuken, L. J. C.; Shenton, C.; Webster, G. R. *Chem. Commun.* **2004**, 316−317.
(43) Friis, E. P.; Andersen, J. E. T.; Madsen, L. L.; Bonander, N.; Møller, P.; Ulstrup, J. *Electrochim. Acta* **1997**, *42*, 2889−2897.
(44) McEvoy, J. P.; Foord, J. S. *Electrochim. Acta* **2005**, *50*, 2933−2941.
(45) Fristrup, P.; Grubb, M.; Zhang, J.-D.; Christensen, H. E. M.; Hansen, A. M.; Ulstrup, J. *J. Electroanal. Chem.* **2001**, *511*, 128−133.
(46) Angerstein-Kozlowska, H. *Comprehensive Treatise of Electrochemistry*; Plenum Press: New York, 1984; Vol. 9.
(47) Conway, B. E.; Angerstein-Kozlowska, H.; Sharp, W. B. A.; Criddle, E. E. *Anal. Chem.* **1973**, *45*, 1331−1336.
(48) Finklea, H. O. *Electroanalytical Chemistry*; Marcel Dekker: New York, 1996; Vol. 19.
(49) van de Kamp, M.; Canters, G. W.; Andrew, C. R.; Sanders-Loehr, J.; Bender, C. J.; Peisach, J. *Eur. J. Biochem.* **1993**, *218*, 229−238.
(50) Bard, A. J.; Faulkner, L. R. *Electrochemical Methods: Fundamentals and Applications*, 2nd ed.; John Wiley and Sons: New York, 2001.
(51) Smith, C. P.; White, H. S. *Anal. Chem.* **1992**, *64*, 2398−2405.
(52) Fujita, K.; Nakamura, N.; Ohno, H.; Leigh, B. S.; Niki, K.; Gray, H. B.; Richards, J. H. *J. Am. Chem. Soc.* **2004**, *126*, 13954−13961.
(53) Bain, C. D.; Troughton, E. B.; Tao, Y.-T.; Evall, J.; Whitesides, G. M.; Nuzzo, R. G. *J. Am. Chem. Soc.* **1989**, *111*, 321−335.
(54) Li, H.; Webb, S. P.; Ivanic, J.; Jensen, J. H. *J. Am. Chem. Soc.* **2004**, *126*, 8010−8019.
(55) Canters, G. W.; Kolczak, U.; Armstrong, F.; Jeuken, L. J. C.; Cambab, R.; Solac, M. *Faraday Discuss.* **2000**, *116*, 205−220.
(56) Lappin, A. G. *Metal Ions in Biological Systems*; Marcel Dekker: New York, 1981; Vol. 13.
(57) Pozdnyakova, I.; Guidry, J.; Wittung-Stafshede, P. *J. Biol. Inorg. Chem.* **2001**, *6*, 182−188.
(58) Leckner, J.; Bonander, N.; Wittung-Stafshede, P.; Malmström, B. G.; Karlsson, B. G. *Biochim. Biophys. Acta* **1997**, *1342*, 19−27.
(59) Fuentes, L.; Oyola, J.; Fernández, M.; Quiñones, E. *Biophys. J.* **2004**, *87*, 1873−1880.
(60) Winkler, J. R.; Wittung-Stafshede, P.; Leckner, J.; Malmström, B. G.; Gray, H. B. *Proc. Natl. Acad. Sci. U.S.A.* **1997**, *94*, 4246−4249.
(61) Wittung-Stafshede, P.; Hill, M. G.; Gomez, E.; Di Bilio, A. J.; Karlsson, B. G.; Leckner, J.; Winkler, J. R.; Gray, H. B.; Malmström, B. G. *J. Biol. Inorg. Chem.* **1998**, *3*, 367−370.
(62) Hwang, H. J.; Ang, M. C.; Lu, Y. *J. Biol. Inorg. Chem.* **2004**, *9*, 489−494.
(63) Katz, E.; Lioubashevsky, O.; Willner, I. *J. Am. Chem. Soc.* **2004**, *126*, 15520−15532.
(64) Nahir, T. M.; Bowden, E. F. *Langmuir* **2002**, *18*, 5283−5286.
(65) Sagara, T.; Niwa, K.; Sone, A.; Hinnen, C.; Niki, K. *Langmuir* **1990**, *6*, 254−262.
(66) Laviron, R. *J. Electroanal. Chem.* **1979**, *101*, 19−28.
(67) Marcus, R. A. *J. Chem. Phys.* **1956**, *24*, 966−978.
(68) Marcus, R. A. *J. Chem. Phys.* **1965**, *43*, 679−701.
(69) Weber, K.; Creager, S. E. *Anal. Chem.* **1994**, *66*, 3164−3172.
(70) Zhao, J. W.; Dong, S. J.; Liu, Z. F. *Chin. J. Anal. Chem.* **2000**, *28*, 661−665.
(71) Marcus, R. A.; Sutin, N. *Biochim. Biophys. Acta* **1985**, *811*, 265−322.
(72) Murgida, D. H.; Hildebrandt, P. *J. Am. Chem. Soc.* **2001**, *123*, 4062−4068.
(73) Avila, A.; Gregory, B. W.; Niki, K.; Cotton, T. M. *J. Phys. Chem. B* **2000**, *104*, 2759−2766.
(74) Yue, H.; Khoshtariya, D.; Waldeck, D. H.; Grochol, J.; Hildebrandt, P.; Murgida, D. H. *J. Phys. Chem. B* **2006**, *110*, 19906−19913.
(75) Engelkes, V. B.; Beebe, J. M.; Frisbie, C. D. *J. Am. Chem. Soc.* **2004**, *126*, 14287−14296.
(76) Weber, K. S.; Hockett, L. A.; Creager, S. E. *J. Phys. Chem. B* **1997**, *101*, 8286−8291.
(77) Hong, H.-G.; Park, W. *Langmuir* **2001**, *17*, 2485−2492.
(78) Murgida, D. H.; Hildebrandt, P. *Phys. Chem. Chem. Phys.* **2005**, *7*, 3773−3784.
(79) Jeuken, L. J. C. *Biochim. Biophys. Acta Bioeng.* **2003**, *1604*, 67−76.
(80) Wei, J.; Liu, H.; Dick, A. R.; Yamamoto, H.; He, Y.; Waldeck, D. H. *J. Am. Chem. Soc.* **2002**, *124*, 9591−9599.
(81) Napper, A. M.; Liu, H.; Waldeck, D. H. *J. Phys. Chem. B* **2001**, *105*, 7699−7707.
(82) Chi, Q.; Farver, O.; Ulstrup, J. *Proc. Natl. Acad. Sci. U.S.A.* **2005**, *102*, 16203−16208.
(83) Messerschmidt, A. *Struct. Bonding* **1998**, *90*, 37−68.

(84) Shepard, W. E. B.; Anderson, B. F.; Lewandoski, D. A.; Norris, G. E.; Baker, E. N. *J. Am. Chem. Soc.* **1990**, *112*, 7817−7819.
(85) Vallee, B. L.; Williams, R. J. P. *Proc. Natl. Acad. Sci. U.S.A.* **1968**, *59*, 498−505.
(86) Williams, R. J. P. *Eur. J. Biochem.* **1995**, *234*, 363−381.
(87) Gray, H. B.; Malmström, B. G. *Comments Inorg. Chem.* **1983**, *2*, 203−209.
(88) Malmström, B. G. *Eur. J. Biochem.* **1994**, *223*, 711−718.
(89) Paraskevopoulos, K.; Sundararajan, M.; Surendran, R.; Hough, M. A.; Eady, R. R.; Hillier, I. H.; Hasnain, S. S. *Dalton Trans.* **2006**, 3067−3076.
(90) Liu, Y. P.; Newton, M. D. *J. Phys. Chem. B* **1994**, *98*, 7162−7169.
(91) Cascella, M.; Magistrato, A.; Tavernelli, I.; Carloni, P.; Rothlisberger, U. *Proc. Natl. Acad. Sci. U.S.A.* **2006**, *103*, 19641−19646.
(92) Ryde, U.; Olsson, M. H. M. *Int. J. Quantum Chem.* **2001**, *81*, 335−347.
(93) Olsson, M. H. M.; Ryde, U.; Roos, B. O. *Protein Sci.* **1998**, *7*, 2659−2668.
(94) Fraga, E.; Webb, A.; Loppnow, G. R. *J. Phys. Chem. B* **1996**, *100*, 3278−3287.
(95) Muegge, I.; Qi, P. X.; Wand, A. J.; Chu, Z. T.; Warshel, A. *J. Phys. Chem. B* **1997**, *101*, 825−836.
(96) Kalverda, A. P.; Ubbink, M.; Gilardi, G.; Wijmenga, S. S.; Crawford, A.; Jeuken, L. J. C.; Canters, G. W. *Biochemistry* **1999**, *38*, 12690−12697.
(97) Jeuken, L. J. C.; Wisson, L.-J.; Armstrong, F. A. *Inorg. Chim. Acta* **2002**, *331*, 216−223.
(98) Crane, B. R.; Di Bilio, A. J.; Winkler, J. R.; Gray, H. B. *J. Am. Chem. Soc.* **2001**, *123*, 11623.
(99) Moore, G. R.; Pettigrew, G. W. *Cytochromes c: Evolutionary, Structural and Physiochemical Aspects*; Springer-Verlag: Berlin/Heidelberg, 1990.
(100) Battistuzzi, G.; Borsari, M.; Canters, G. W.; de Waal, E.; Loschi, L.; Warmerdam, G.; Sola, M. *Biochemistry* **2001**, *40*, 6707−6712.